The Effect of Plasma Spraying on the Microstructure and Aging Kinetics of the Al-Si Matrix Alloy and Al-Si/SiC Composites

Yahya Altunpak, Hatem Akbulut, and Fatih Üstel

The Al-Si (LM 13)-based matrix alloy reinforced with SiC particles containing 10, 20, and 30 vol.% SiC particles were spray-formed onto Al-Si substrates. The sprayed samples were directly subjected to a standard aging treatment (T551). From the experiments, it was observed that the high rate of solidification resulted in very fine silicon particles which were observed as continuous islands in the matrix and each island exhibited several very fine silicon crystals. Analysis showed that plasma-spraying caused an increased solid solubility of the silicon in the aluminum matrix. DSC measurements in the permanent mold-cast Al-Si matrix alloy and plasma-sprayed Al-Si matrix alloy showed that plasma-spraying causes an increase in the amount of GP-zone formation owing to the very high rate solidification after plasma-spraying. In the plasma-sprayed Al-Si/SiC composites GP zones were suppressed, since particle-matrix interfaces act as a sink for vacancies during quenching from high plasma process temperature. Introduction of SiC particles to the Al-Si age-hardenable alloy resulted in a decrease in the time required to reach plateau matrix hardness owing to acceleration of aging kinetics by ceramic SiC particles.

Keywords	aging kinetics, MMCs, plasma spraying, wear

1. Introduction

Composite materials can bring the combined advantages of both reinforcement and matrix materials into full play, which gives us quite a high degree of freedom in material design. The study of composite materials has, therefore, become one of the frontiers in materials science research, especially the study of metal matrix or intermetallics matrix composites (Ref 1). There are, however, problems associated with the application of conventional processing techniques for metal matrix composites (MMCs). Among them, the compatibility between the reinforcement and the matrix is often cited as a chief concern. There are a number of production methods for MMCs, and each of these methods has certain advantages coupled with disadvantages. The oldest method of manufacturing is the powder metallurgy route. This has all the advantages of a well-known and mature technology, but it is relatively expensive because of the large number of steps in the overall process. Two further disadvantages are the possibility of segregation of powder because of density or size differences, and the fact that many desirable combinations are not possible (Ref 2). Melt-processing is an alternative and attractive procedure in certain cases. This method is simple and cheap when compared with other manufacturing processes. This method is only applied to certain systems where long contact times at high temperatures can be tolerated without deterioration of the composite (Ref 3). Plasma-spraying of the metal and ceramic powder mixtures is an alternative new MMC production technique for elimination of the deleterious effect of the interface phases. Gui and co-workers (Ref 4-6) studied different series of the SiCp-reinforced aluminum composites with plasma-spraying process. They pointed out that no reaction products or oxidation were observed in the resultant composite materials. They also reported that such composites are good candidates for electronic packaging, wear and high temperature applications.

In this study, Al-Si matrix alloy containing SiC particles is intended to coat a monolithic Al-Si matrix alloy substrate by plasma-spraying technique to eliminate the liquid-SiC interaction time and to obtain a thick layer with good wear resistance and homogenous particle distribution.

2. Experimental Details

The Al-Si/SiC composites were produced by a thermal plasma-spraying process as thick composite films. Plasma-sprayed matrix was an Al-12wt.%Si, 1.2 wt.%Cu, 0.9 wt.%Mg Al-Si matrix alloy powder. Matrix alloy powders with a grain size range between 30 and 50 μm were mechanically mixed with 10, 20, and 30 vol.% SiC powders so that the particle size range was between 30 and 40 μm. The mechanically mixed unreinforced Al-Si and composite powders were sprayed onto a Al-Si matrix alloy substrate (chemical composition by wt.%: 12 Si, 1.16 Cu, 1.21 Mg, 0.9 Ni, 0.17 Zn, 0.12 Mn, 0.48 Fe, balance Al) with planar geometry in air using a Metco plasma-spray gun with Ar-H$_2$ plasma. The Al-Si powders and the

Yahya Altunpak, Gerede Vocational School of Higher Education, Abant Izzet Baysal University, 14900 Bolu, Turkey; and Hatem Akbulut and Fatih Üstel, Department of Metallurgical and Materials Engineering, Engineering Faculty, Sakarya University, Esentepe Campus, 54187 Sakarya, Turkey. Contact e-mail: yaltunpak@yahoo.com.

Al-Si/SiC mixtures were formed by injection of a mixture of aluminum-silicon alloy and SiC particle powders into the hot plasma zone (8000 to 12,000 °C) of an Ar-H_2 thermal plasma jet.

Although the jet can be extremely hot, powder-injection parameters and residence time inside the jet were controlled so that only the Al-Si alloy powder would melt. This selective melting was controlled by adjustment of the current at 500 A, voltage between anode and cathode 60 to 70 V, and H_2 and Ar flow rates 10 and 60 sccm, respectively. The ceramic particles remained in solid state and no melted SiC particle was detected after the spraying process. After the plasma-spray deposition process, the samples were directly subjected to a standard aging treatment (T551) up to 60 h at 204 °C. A standard gravity-cast Al-Si matrix alloy was also produced for the comparison of the aging characteristics with the plasma-sprayed Al-Si matrix alloy. For gravity-cast unreinforced alloy a permanent cast iron mold, which was heated up to 150 °C, was used and the melt superheated to 700 °C prior to casting. After the casting process, the mold was water-quenched. Porosity and the amount of the retained SiC particles of the coatings were measured by means of a line-intercept method with an optical microscope equipped with an image analysis system.

Microhardness measurements were carried out with a LECO M-400 microhardness tester. A micro-Vickers microhardness indenter was used to provide indentation depths in the sprayed layers. A 50 g load was applied for 15 s to measure the hardness. Optical microscopy, scanning electron microscopy (SEM), and x-ray analysis were carried out for both as-sprayed and as-cast specimens. Energy dispersive spectroscopy (EDS) analysis was performed from Si and SiC-free regions in a Cambridge Ins. Stereoscan SEM attached to a 360 Noran EDS energy dispersive spectroscopy facility. Analysis was carried out in both the unreinforced gravity-cast Al-Si matrix alloy and plasma-sprayed matrix materials. Plasma-sprayed materials and the gravity-cast Al-Si matrix alloys were immediately stored in a −15 °C refrigerator after production of the materials. Discs (5 mm diameter and 0.3 mm thickness) for differential scanning calorimetry (DSC) were polished and weighed. The DSC analysis of rapid-quenched matrix alloy and composites were carried out with a Perkin-Elmer DSC 1700 thermal analyzer. Disc samples were loaded into a DSC cell at room temperature and equilibrated for a few minutes. The heating rate was 10 °C/min from 25 to 550 °C. Dry pure nitrogen was purged through the cell at the rate of 55 mL/min to avoid oxidation. The data for all the DSC runs were recorded in the instrument memory. At the last two samples were analyzed for each heat-treated material. Dry ball-on disk wear-testing was also performed on the plasma-spray-deposited Al-Si/SiC composites layers. During the test, friction force originating from the normal force was measured by a load-cell (strain gauge) mounted on the loading arm. The wear tests were conducted with a cemented carbide (WC-Co) ball (4.6 mm diameter) sliding against plasma-sprayed coatings. The wear tests were performed in ambient air and in relative humidity (38 to 39%RH) and 24 °C. The wear and friction tests were carried out at 5 N load and at the sliding speed of 0.1 m/s. Width of wear track was measured in the optical microscopy and the wear rate was measured.

3. Results and Discussion

The thermal plasma-spraying technique described in this study was designed to produce Al-Si alloy matrix composites reinforced with ceramic SiC particles to obtain homogenous particle distribution with high wear resistance.

The cross-sectional microstructures of the plasma-sprayed composites are presented in Fig. 1. As seen from the figure,
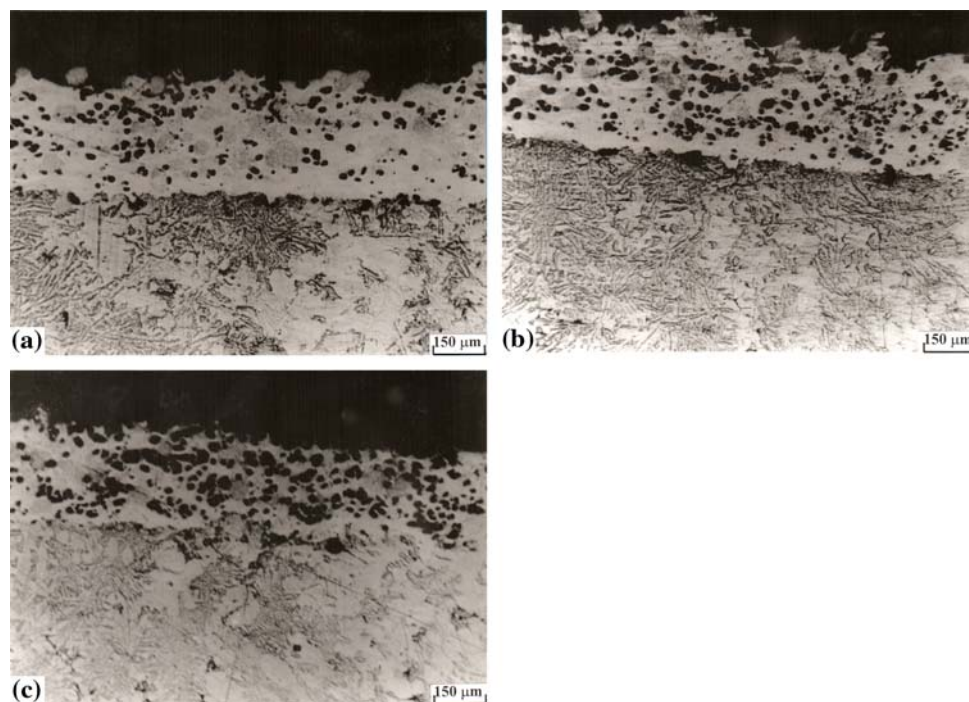

Fig. 1 Cross-sectional microstructures of the plasma-sprayed Al-Si/SiC composites: (a) 10 vol.% SiC, (b) 20 vol.% SiC, and (c) 30 vol.% SiC
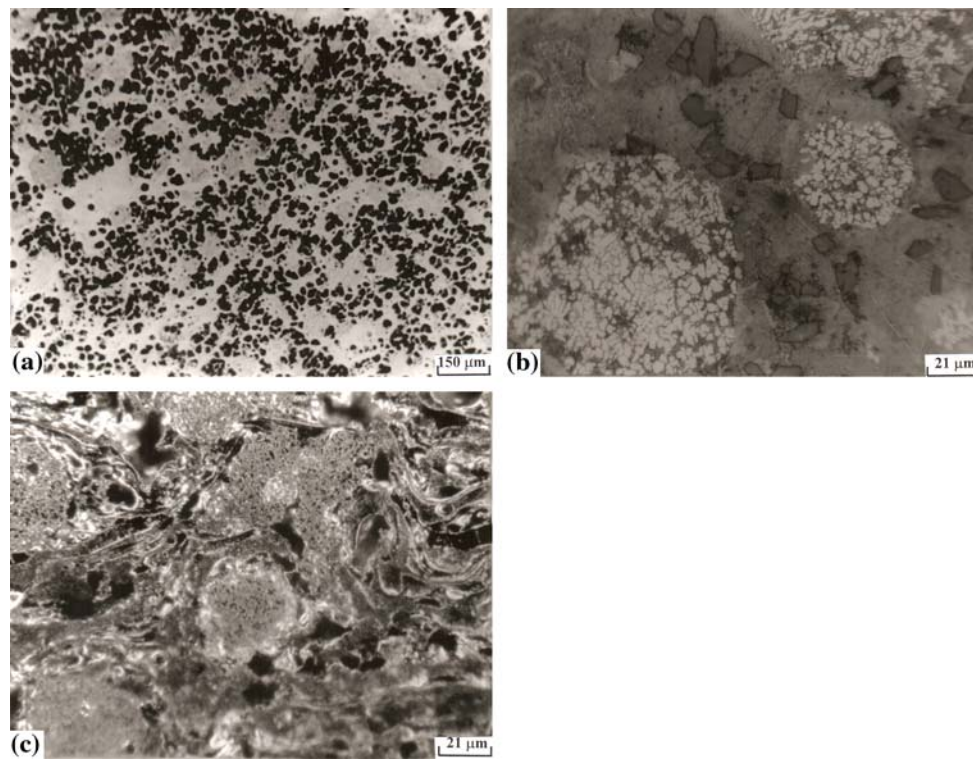
Fig. 2 30 vol.% SiC-reinforced Al-Si matrix alloy: (a) particle distribution, (b) eutectic island (light image), and (c) eutectic island (dark image)

Table 1 A summary of plasma sprayed materials

Sample	Particle volume percent		Coating thickness, μm	Brinell hardness	Porosity, %	Wear rate, 10^{-5} mm^3/m	Friction coefficient
	Added	Measured					
Substrate	...	...	...	86.0	...	...	...
Al-Si(0)	0	0	427.1	95.5	6.1	7.95	0.53
Al-Si(10)	10	7	375.5	136.6	5.2	6.84	0.50
Al-Si(20)	20	17	370.4	161.6	6.6	4.85	0.61
Al-Si(30)	30	26	324.2	168.6	6.2	3.84	0.58

only Al-Si alloy was melted by the plasma heat and the SiC particles remained in an unmelted state. Figure 1 also shows that the matrix microstructure of plasma-sprayed layer and the substrate is significantly different. In the gravity-cast alloy and in the substrate material, the eutectic silicon crystals have a coarse lamellar morphology, but plasma-sprayed materials reveal totally different silicon crystals. Eutectic silicon crystals are observed as equiaxed fine particles that are segregated in the form of continuous islands. Figure 2, on the other hand, shows the particle distribution (Fig. 2a) of the eutectic island in high magnification (Fig. 2b) and, dark-field image (Fig. 2c) of the 30 vol.% SiC reinforced material. Some of the important properties of the substrate material and the plasma-sprayed Al-Si/SiC composite are summarized in Table 1. As can be seen from the table, the particle volume fraction showed a high retention ratio after plasma-spraying on the Al-Si matrix alloy substrate. Table 1 also shows the experimental results such as Brinell Hardness, porosity, sprayed layer thickness, wear rate, and friction coefficient in the unreinforced matrix and its composites.

In recent years, the incorporation of ceramic particles into aluminum matrix composites has gained considerable interest (Ref 7). Traditional production techniques for SiC-ceramic-reinforced MMCs have limited use because of a high rate of chemical interaction between SiC and aluminum matrix. Powder metallurgy, osprey, and thermal-spraying techniques are alternative methods of decreasing this interaction between the composite constituents (Ref 8). The microstructure of plasma-sprayed Al-Si matrix alloy and composites showed significant differences when compared with gravity-cast alloy. Plasma-sprayed Al-Si matrix alloy and composites have large amounts of primary aluminum-rich solidification structure owing to rapid solidification behavior. The eutectic phase in the sprayed materials accumulated in the form of continuous islands with very fine silicon particles. Eutectic precipitation was observed between primary α-dendrite arms. Two facts are evident. One is that fine structures are not flake-like in form but fibrous. In brief, the structure was quench-modified. The second one is that the coupled zone in this system is asymmetric and even if silicon content is very high α-dendrites
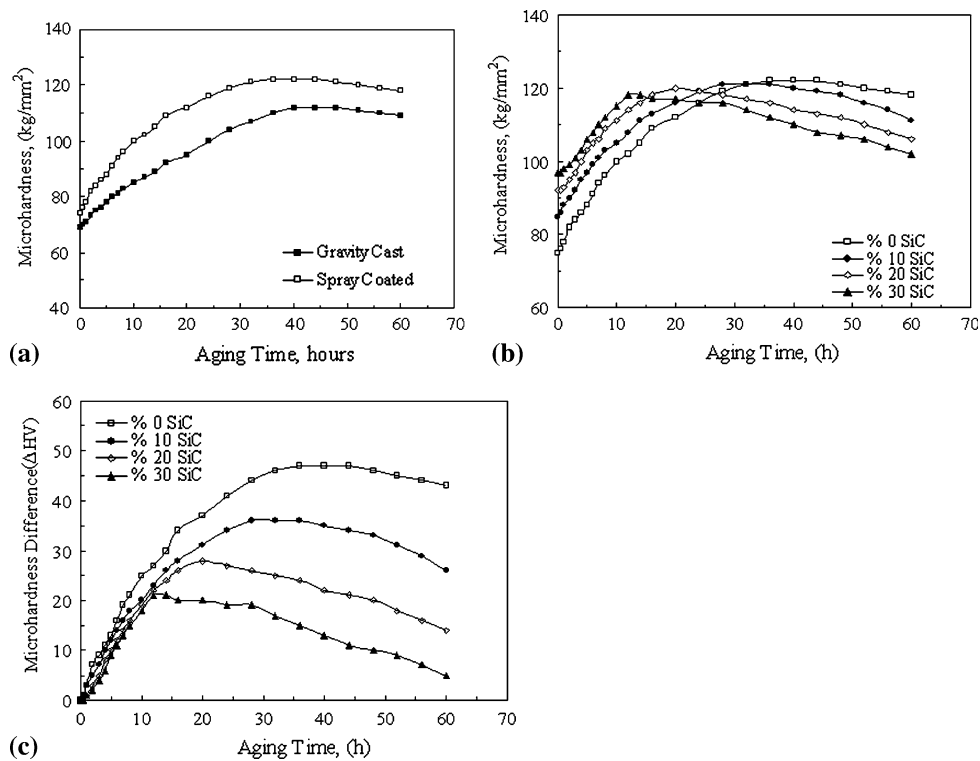
Fig. 3 (a) Vickers microhardness variation with aging time at 204 °C aging temperature in a gravity-cast and plasma-spray coating of Al-Si matrix alloys, (b) Microhardness-aging time relationship in plasma-sprayed materials, and (c) Microhardness difference with aging time

always forms. This effect has been explained for eutectic metal systems (Ref 9).

The hardness measurements obtained for the gravity-cast and plasma-spray deposited matrix alloy that were subjected to a standard T551 heat treatment are shown in Fig. 3(a). As can be clearly seen, the plasma-sprayed matrix alloy produced higher hardness values compared with the gravity-cast matrix alloy. Figure 3(b) and (c), on the other hand, presents the microhardness results of the plasma-sprayed matrix alloy and SiC-particle-reinforced composites upon aging time. Figure 3(b) shows the microhardness data taken from the primary α-Al dendrites (SiC and Si-free regions) for the SiC-particle-reinforced composites and shows that increasing the particle volume ratio in the Al-Si matrix alloy resulted in a decrease of the peak aging time. Figure 3(c) presents the microhardness differences obtained by aging treatment compared with as produced state (rapid-quenched or solutionized state). The microhardness increment of unreinforced matrix alloy is obtained as 47 HV at the maximum peak-hardness time of 40 h. Incorporation of SiC particles into Al-Si matrix alloy resulted in a decrease of the hardness increment and peak aging time. For example, the maximum microhardness of 30 vol.% SiC-particle-reinforced composite material showed 21 HV hardness increment in 14 h aging time, which is the peak aging condition. This increment is 47 HV in the unreinforced alloy at 40 h peak aging time.

The aging behavior of MMCs with age-hardenable alloy matrix can affect the heat-treatment behavior and the final application properties, so that it has become the subject of much interest (Ref 1, 10). The comparison between gravity cast and plasma-sprayed Al-Si matrix alloys showed that plasma-sprayed materials exhibited higher microhardness values. This

was attributed to emanation of eutectic from rapid quenching. Because of the rapid quenching, high dislocation density can be obtained in the plasma-sprayed materials. Another reason is the higher solid solubility of silicon by the α-aluminum dendrites in plasma-sprayed materials, as evidenced by the EDS and x-ray analysis. A very high rate of solidification should affect the curvature on the equilibrium diagram, and α-dendrites dissolve much more silicon than conventionally solidified alloys. Wermolen et al. (Ref 11) have also stated that the dissolution kinetics of Si particles in an aluminum alloy can be altered with changing thermodynamic driving forces. The hardening response of the plasma-sprayed Al-Si matrix alloy containing high volume fractions of SiC particles degraded sharply, and the lowest increase in the Vickers hardness value, upon heat treatment, obtained in the 30 vol.% SiC-contained plasma-sprayed material. The results indicate that the fall in the hardening response of the composites, with increasing volume percent of the SiC particles, was much faster than expected. The same results have been observed in the short alumina fiber-reinforced Al-Si-Cu alloys (Ref 12). In this study, the age-hardening condition was kept constant for the matrix alloy and the plasma-sprayed composites. It may be possible to increase, or even to do away with the peak in hardness by exploration of hardening conditions for each SiC particle volume, as Thomas and King (Ref 13) showed for SiCp-reinforced 2124 Al alloy. T551 standard heat-treatment studies proved that plasma-sprayed matrix alloy was more suitable for aging treatment than gravity-cast alloy, which has almost the same chemical composition as sprayed Al-Si matrix alloy. Because of the very high rate of solidification (i.e., 10^4 °C/s) by plasma process, the Al-Si matrix alloy remained nearly in the solid solution state. This resulted in more effective precipitation reaction than

gravity-cast Al-Si matrix alloy. It is reported by Zhang et al. (Ref 1) and Thomas and King (Ref 13) that in MMCs with heat-treatable matrix the already-existing intermetallic phases could not be completely dissolved into matrix during solutionizing treatment. After quenching from the solutionizing temperature, therefore, the amount of precipitated phase was reduced. In plasma-sprayed matrix, the hardening at higher cooling rates is because of vacancy/GP zones and dislocations. As the cooling rate increases, the amount of quenched-in vacancies necessary for GP-zone formation also increases. Because of the high cooling rates, the amount of quenched-in vacancies available for precipitation and solute strengthening is increased in the plasma-sprayed matrix alloy.

The DSC traces of the unreinforced Al-Si matrix and the SiC-particle-reinforced composite materials are shown in Fig. 4. For comparison purposes, results from DSC scans of the gravity-cast Al-Si matrix alloy and plasma-sprayed Al-Si matrix alloy are presented in Fig. 4(a). The DSC traces of matrix alloys produced by gravity-cast and plasma-spraying do not exhibit significant differences depending on the GP-zone formation/dissolution and precipitate formation/dissolution temperatures. The curve of Al-Si matrix alloys shows the exothermic reaction between 45 to 47 °C and 137 to 140 °C owing to the formation of GP zones; the endothermic between 137 to 140 °C and 238 to 240 °C owing to the dissolution of GP zones; the exothermic between 238 to 240 °C and 361 to 363 °C owing to formation of precipitates; and the endothermic between 361 to 363 °C and 481 to 486 °C owing to dissolution of precipitates. The DSC curve for gravity-cast matrix material, however, exhibits smaller amounts of GP-zone formation compared with plasma-sprayed matrix alloy. From the DCS curves, another obvious difference to note is that the plasma-sprayed matrix exhibits two precipitate peaks (marked A and B),

whereas the gravity-cast matrix shows only a single precipitate peak (marked B). Figure 4(b) shows the DSC curves for the plasma-sprayed Al-Si matrix reinforced with SiC particles. Figure 4(b) reveals that introducing SiC particles into the Al-Si matrix alloy results in a suppression of GP-zone formation. Among the SiC particle composites studied only the 10 vol.% SiC-reinforced Al-Si matrix alloy shows a small GP-zone formation peak. Excess SiC particles result in the disappearance of GP zones in the matrix. As can be seen from Fig. 4(b), reinforcing the Al-Si matrix alloy by SiC particles causes acceleration of precipitate formation. The peaks identified in Fig. 4(b) and the corresponding temperatures are presented in Table 2.

The hardness versus aging time and the DSC curves show similar trends between the gravity-cast and plasma-sprayed matrix materials. There is no clear indication that the time to peak hardness is affected by quench rate. Plasma-sprayed matrix alloy produced more GP zones when compared with gravity-cast material. Increasing the amount of GP zones in the plasma-sprayed matrix resulted in a higher amount of precipitates in the plasma-sprayed matrix material. Couper and Polmear (Ref 14) have also suggested that increasing the amount of quenched-in vacancies facilitates nucleation of precipitates during aging. It can be seen that the age-hardening rate of Al-Si matrix material is affected by the presence of ceramic particles.

Plasma-sprayed Al-Si matrix that is reinforced with SiC particles does not show GP-zone formation, except that 10 vol.% SiC-reinforced composite revealed a small amount of GP zone area. In the composites, dislocations and matrix-particle interfaces serve as vacancy sinks, which inhibit GP-zone formation, as also stated by several authors (Ref 8, 13, 15). Since a large amount of dislocations is formed in the composite rather
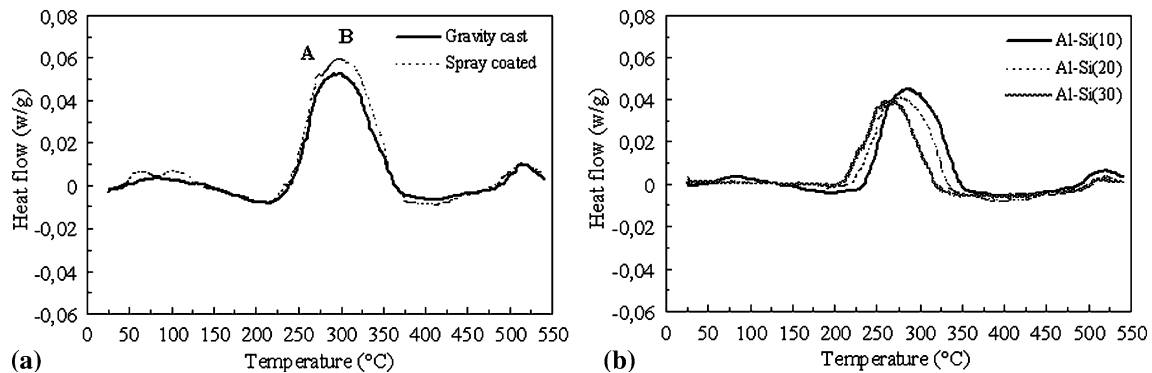

Fig. 4 Results of DSC analysis: (a) Al-Si matrix alloys and (b) Plasma-sprayed Al-Si/SiC composites

Table 2 Analysis of DSC scans of matrix material and composites

Material	Temperature of the peaks, °C				
	GP-zone formation	GP-zone dissolution	Precipitate formation	Peak for precipitate	Precipitate dissolution
Gravity-cast LM 13	45	140	240	297	363
Plasma-sprayed LM 13	47	137	238	299	361
LM + 10 vol.% SiC	52	132	235	288	348
LM + 20 vol.% SiC	...	...	220	277	331
LM + 30 vol.% SiC	...	...	205	262	318

than quenched-in vacancies and the GP zones, the time required to attain peak aging is decreased when compared with unreinforced alloy. Hardness and DSC curves of the composites indicated that particles accelerated the aging kinetics of the Al-Si matrix material.

The solid solubility of Si in Al is approximately 1.9 wt.% at 570 °C. In equilibrium state, the solid solubility of Si in Al is omitted. Increasing the cooling rate, however, promotes solubility for solid solution, as is well known. In this study, the EDS analysis taken from the primary α-aluminum dendrites revealed that in plasma-sprayed matrix alloys, more Si was dissolved in the aluminum matrix compared with Si solubility in the gravity-cast matrix alloy. The EDS analysis showed that approximately 0.5 wt.% Si was detected in α-Al primary phase whereas in plasma-sprayed unreinforced alloy Si content was measured as 1.1 wt.%. Similar analysis is valid for Cu dissolution. Since an increase was observed in the solid solubility of Si in the α-Al primary phases, x-ray analysis was carried out to reveal enough evidence by obtaining lattice parameters. The stored gravity-cast and plasma-sprayed matrix materials at refrigerator (at −15 °C) were x-ray analyzed and the obtained lattice parameters are summarized in Table 3. It is clearly seen from the table that plasma-sprayed matrix alloy produced smaller lattice parameters than those of gravity-cast matrix alloy.

Figure 5 shows the x-ray diffraction patterns for the gravity-cast and plasma-sprayed Al-Si matrix alloy after 30 h aging at 204 °C. The gravity-cast material shows only a S′ Al_2CuMg precipitate (pattern a). It can be seen from the x-ray patterns of the plasma-sprayed matrix material that an additional precipitated phase in the Mg_2Si type is found in the matrix (pattern b).

In this study, the plasma-spraying process caused to retain more alloying elements in the matrix and eliminated the adverse effects emanating from composite matrices. Moreover, a very high rate of solidification reaction eliminated

solutionizing of the matrix, and this is another attractive feature to decrease the cost of the alloy production. The x-ray analyses performed for Al-Si plasma-sprayed matrix alloy and the plasma-sprayed SiC-containing composites have shown that thermal treatment yields the formation of β and S′-type precipitates for both matrix alloy and its composites, whereas gravity-cast matrix material shows only S′-type precipitates. This was attributed to more Si dissolution owing to a very high rate of solidification in the plasma-sprayed matrix and its composites. Additional β′ (Mg_2Si) precipitates therefore were formed in the plasma-sprayed materials.

Moreover, as-sprayed Brinell hardness values are listed in the table, as well. After the ball-on disk wear-testing with 0.5 m/s sliding speed at 5 N applied normal load at the dry condition in air, wear resistance of the SiC-particle-distributed Al-Si matrix alloy was also increased almost linearly with increasing SiC particle content, but a small increment was detected in the friction coefficient values.

In accordance with the high cooling rate, the wear resistance values and the coefficient of friction values were seen to be quite satisfactory for plasma-sprayed materials (shown in Table 1). For the composites, SiC particles have higher hardness and wear resistance than the matrix. During the wear process, the matrix material will be worn off rapidly, and the homogenously distributed SiC particles will bear the load, which will retard the wear process and result in a finer wear trace on the surface. As obtained from the wear results, increasing particle content in the plasma-sprayed Al-Si/SiC composite resulted in a decrease in the wear rates. As also stated by Ghost et al. (Ref 16) plasma-spraying process can obtain very homogeneous particle distribution without clustering even at the 50 to 60 vol.% particle addition, and this decreases the wear rate almost linearly with increasing particle volume. Wielage et al. (Ref 17), consistent with this study, found that thermal plasma-spraying has a main advantage in terms of superior tribological properties of materials, and thus this coating structure opens a wide field of technological applications.

Table 3 Lattice parameters in the gravity cast and plasma spray produced matrix materials

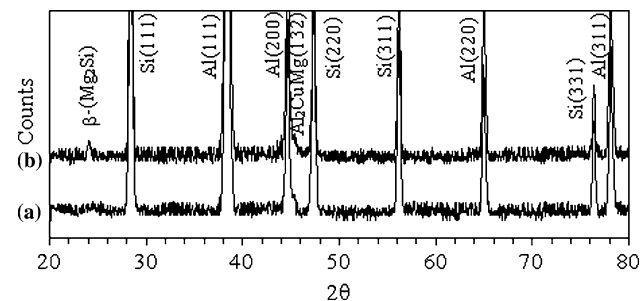| Matrix material	2θ	d, Å	hkl	a, Å
Gravity cast	38.40	2.3421	111	4.0567
	44.64	2.0281	200	4.0563
Plasma sprayed	65.02	1.4331	220	4.0536
	38.46	2.3386	111	4.0510
	44.72	2.0247	200	4.0494
	65.11	1.4316	220	4.0492

Fig. 5 XRD patterns for 30 h aged materials at 204 °C: (a) 30 vol.% SiC particle contained Al-Si matrix alloys and (b) Unreinforced Al-Si matrix alloy

4. Conclusions

1. The Al-Si matrix alloy containing SiC-ceramic particles can be produced by plasma-spray method on the metal substrates for high wear-resistance applications.
2. Very high rate of solidification after plasma-spraying increased the solid solubility of the alloying elements in the matrix, and this caused an increase in the hardness compared with gravity-cast material.
3. Effective solid solubility by plasma-spraying process can eliminate the solutionizing process and obtain higher hardness for the matrix when compared with traditional casting processes.
4. Incorporation of SiC particles into Al-Si matrix alloy resulted in changed precipitation kinetics. Increasing particle volume content in the matrix accelerated precipitation reaction and caused over-aging when compared with unreinforced plasma-sprayed matrix.
5. Although having an approximate 6% porosity level, the wear resistance increases with the addition of SiC particles, with a small amount of increment in the coefficient of friction.

References

1. J.S. Zhang, X.J. Liu, and H. Cui, Microstructure and Properties of Spray-Deposited 2014 + 15 vol. pct SiC Particulate-Reinforced Metal Matrix Composite, *Metall. Trans.*, 1997, **28A**, p 1261–1269

2. A.R.E. Singer, Metal Matrix Composites made by Spray Forming, *Mater. Sci. Eng.*, 1991, **A135**, p 13–17

3. S. Dallaire and J.G. Legoux, High-Temperature Tribological Properties of Plasma-Sprayed Metallic Coatings Containing Ceramic Particles, *J. Therm. Spray Technol.*, 1996, **5**, p 43–48

4. M. Gui, S.B. Kang, and K. Euh, Microstructure Characteristics of SiC Particle-Reinforced Aluminum Matrix Composites by Plasma Spraying, *J. Therm. Spray Technol.*, 2004, **13**, p 537–543

5. M. Gui and S.B. Kang, Dry Sliding Wear Behavior of Plasma-Sprayed Aluminum Hybrid Composite Coatings, *Metall. Trans.*, 2001, **32A**, p 2383–2392

6. M. Gui, S.B. Kang, and K. Euh, Influence of Spraying Conditions on Microstructures of Al-SiCp Composites by Plasma Spraying, *Metall. Trans.*, 2005, **36A**, p 2471–2480

7. S. Su, X. Liang, A. Moran, and E.J. Lavernia, Solidification Behavior of an Al-6Si Alloy During Spray Atomization and Deposition, *Int. J. Rapid Solid.*, 1994, **8**(3), p 161–177

8. E.J. Lavernia, J.D. Ayers, and T.S. Srivatsan, Rapid Solidification Processing with Specific Application to Aluminum-Alloys, *Int. Mater. Rev.*, 1992, **37**, p 1–37

9. O.A. Atasoy, F. Yilmaz, and R. Elliott, Growth Structures in Aluminium-Silicon Alloys I. The Coupled Zone, *J. Cryst. Growth*, 1984, **66**, p 137–146

10. Y. Song and T.N. Baker, Accelerated Aging Processes in Ceramic Reinforced AA-6061 Composites, *Mater. Sci. Technol.*, 1994, **10**, p 406–413

11. F.J. Wermolen, H.M. Slabbekoorn, and S. Van De Zwang, The Apparent Activation Energy for the Dissolution of Spherical Si-Particles in AlSi-Alloys, *Mater. Sci. Eng.*, 1997, **A231**, p 80–89

12. H. Akbulut, M. Durman, and F. Yilmaz, A Comparison of As-Cast and Heat-Treated Properties in Short Fiber Reinforced Al-Si Piston Alloys, *Scr. Mater.*, 1997, **36**, p 835

13. M.P. Thomas and J.E. King, Effect of Thermal and Mechanical Processing on Tensile Properties of Powder Formed 2124 Aluminium and 2124 Al-SiCp Metal Matrix Composites, *Mater. Sci. Technol.*, 1993, **9**, p 742–753

14. M.J. Couper and I.J. Polmear, Quench Sensitivity in Some Rapidly Solidified Aluminum-Alloys, *J. Mater. Sci. Lett.*, 1987, **6**, p 922–925

15. N.A. Oguocha, M. Radjabi, and S. Yannacopoulso, The Effect of Cooling Rate on the Quench Sensitivity of 2618 Al/Al$_2$O$_3$ MMC, *J. Mater. Sci.*, 2000, **35**, p 5629–5634

16. K. Ghost, T. Troczynski, and A.C.D. Chaklader, Aluminum-Silicon Carbide Coatings by Plasma Spraying, *J. Therm. Spray Technol.*, 1998, **7**, p 78–86

17. B. Wielage, S. Steinhauser, T. Schnick, and D. Nickelmann, Characterization of the Wear Behavior of Thermal Sprayed Coatings, *J. Therm. Spray Technol.*, 1999, **8**, p 553–558